NZE 31-(EQC 1991/37)

Foreshocks of the 1990 Tennyson & Weber Earthquakes - Could they have been recognised?

T H Webb, IGNS

NZE 6

91/37

NZE 006 (31)

Bulletin of the Seismological Society of America, Vol. 84, No. 6, pp. 1739–1753, December 1994

Spatial Clustering and Stress Drops of Foreshocks of the February 1990 Tennyson and Weber, New Zealand, Earthquakes

by Terry H. Webb

Abstract The ability to distinguish foreshocks from background seismicity is very important in short-term earthquake prediction. To that end we have looked at spatial clustering (using waveform cross-correlation) and stress drops of foreshocks of two New Zealand earthquake sequences that occurred in 1990. The Tennyson sequence, located in a continental margin-type strike-slip environment, consisted of a group of foreshocks, an $M_L = 5.8$ mainshock, and many aftershocks. A cross-correlation analysis showed five spatially close clusters of activity prior to the mainshock. Two were event pairs located within the final aftershock zone, two were clusters of four events, each located outside the aftershock zone, and the fifth was a cluster of eight immediate foreshocks located within the aftershock zone. An analysis of two nearby control regions showed that pairs of identical events were not uncommon, but larger clusters were. Stress drops of three events in the 12 days before the mainshock, obtained by deconvolving small events as empirical Green's functions, were lower than for earlier preshocks and aftershocks. Source time functions derived from the Green's function deconvolution indicated that a unilateral rupture model was more appropriate than a circular source model.

Cross-correlation values from the $M_L = 5.9$ Weber sequence also showed spatial clustering, but this was well removed from the mainshock in space and time. A control area also showed similar clustering, suggesting that it is a normal feature of the seismicity at a convergent margin. The Weber foreshocks, only four in all, were not highly correlated. For both sequences, foreshocks did not correlate with the aftershocks, indicating that they occurred in a region of complete coseismic stress relief.

A stress drop of 1650 bars was obtained for a 44-km-deep event that occurred within the upper part of the subducting Pacific Plate, nearby, but not related to the Tennyson sequence.

Introduction

The ability to distinguish foreshocks from normal background seismicity is very important in short-term earthquake prediction. There are various possible ways of recognizing foreshocks, prior to the occurrence of their mainshock, ranging from statistical analysis of precursory seismicity through to detailed analysis of the source parameters of individual events. In this study we adopt the latter approach, in that we look for spatial clustering of foreshocks using waveform cross-correlations. Then, where possible, we derive stress drops of foreshocks, selected aftershocks, and other events that are part of the normal background seismicity by using small, nearly identical events as empirical Green's functions. In this article we consider a foreshock, whether it can be recognized beforehand or not, to be an earthquake that occurs within 30 days of a larger event (Smith, 1981) and within the location uncertainty of the final rupture zone. Preshocks are similarly defined, but within 2 yr of the main event.

New Zealand has recently experienced several moderate ($5.6 < M_L < 6.2$) earthquakes, some of which had foreshocks. For the first time, small to large foreshocks, mainshocks, and aftershocks have been recorded on scale on the new N.Z. National Seismograph Network digital EARSS stations (Gledhill *et al.*, 1991). While the average station spacing of about 100 km is relatively large compared with dense telemetered networks such as in California, the good sites obtainable by the fact that stations do not need to be sited for radio telemetry, and high-quality instrumentation, mean that the regional waveforms so recorded are suitable for this kind of study. In addition, large events have occurred in both a continental-type strike-slip environment (Tennyson, 10 February 1990, $M_L = 5.8$) and at a subduction zone (Weber, 19 February 1990, $M_L = 5.9$) (Fig. 1).

Foreshocks have been intensively studied by many people. Of relevance to this study, which concentrates on spatial clustering, is the work of Ishida and Kanamori (1978), who observed high similarity between waveforms for preshocks of the 1971 San Fernando earthquake, but noted that these preshocks differed from both the mainshock and aftershocks. Waveform similarity at given stations indicates that events occur within a one-quarter wavelength of each other (Geller and Mueller, 1980; Thorbjarnardottir and Pechmann, 1987). Foreshocks would occur in tight spatial clusters if they were produced by the failure of a small, high-strength asperity (Kanamori, 1981). Pechmann and Kanamori (1982) found that two groups of preshocks in the 2 yr before the 1979 Imperial Valley earthquake also had well-correlated

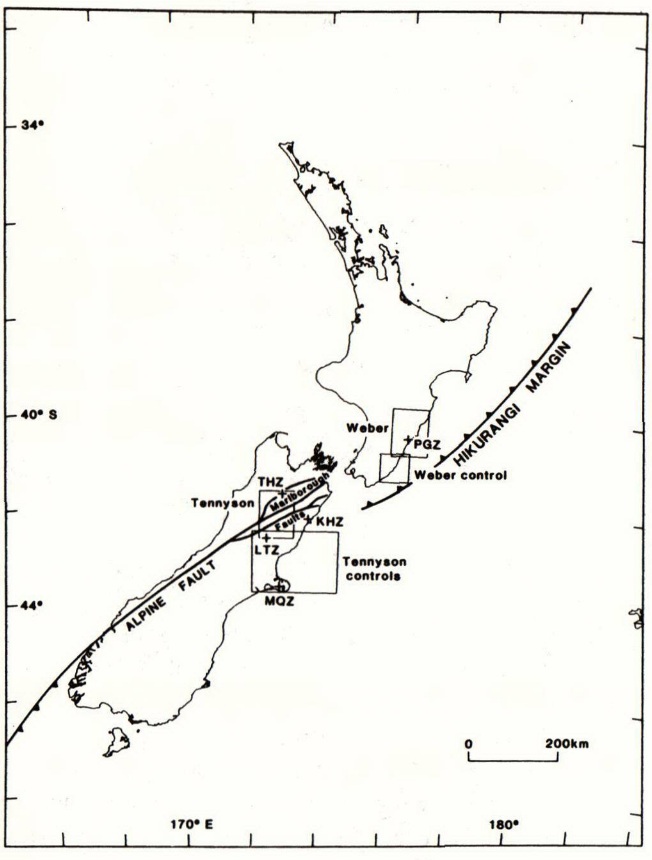

Figure 1. New Zealand and its tectonic setting. Rectangles mark each of the study and control areas discussed in the text. National network seismograph stations used in this study are marked with + symbols.

waveforms. Pechmann and Thorbjarnardottir (1990) studied two Utah earthquake sequences and observed spatial clustering of preshocks 10 months before one mainshock, but not before another. They suggested that the observed clustering could be due to an asperity breaking in a heterogeneous fault zone, while the lack of clustering for the other event may be due to that fault being more homogeneous in terms of strength; i.e., there were no large isolated asperities to be broken. Motoya (1990) has reported that some foreshock sequences show strong similarity, while aftershocks differ from event to event. Such foreshock sequences also have a more sporadic distribution of occurrence in time, distinguishing them from aftershocks.

If foreshocks that exhibit spatial clustering are occurring on asperities on the mainshock fault plane, they should have higher than average stress drops, as weaker regions of the fault will have broken in earlier events (Kanamori, 1981). Ishida and Kanamori (1980) found that foreshocks of the 1952 Kern County, California, earthquake had systematically higher frequency spectral peaks than earlier events within the same region. Tsujiura (1977) examined the spectral features of three foreshock sequences and found significant differences between stress drops of foreshocks and other events, although the differences were not consistent. Frankel (1984) compared the stress drops of two magnitude 5 earthquakes in the Anza seismic gap with that of a 1979 Imperial Valley aftershock by using empirical Green's functions. While the Anza events were not foreshocks, one might have expected their stress drops to be relatively high, as they occurred in a region thought to be due for a large earthquake. Since their stress drops were not unusually high, this implies that either crustal stresses are not high near Anza, or individual stress drops are not reliable indicators of crustal stress. Mori and Frankel (1990) also used empirical Green's function deconvolutions to determine stress drops of earthquakes in the 1986 Palm Springs sequence. One preshock had a relatively high stress drop compared to most, but not all, aftershocks.

In this article we examine, by using cross-correlation techniques, the spatial clustering that occurred in the preshocks and aftershocks of the Tennyson and Weber earthquakes. Where possible, we derive stress drops of preshocks, aftershocks, and other nearby events by deconvolving smaller events, used as empirical Green's functions. In order to get a better idea of how common spatial clustering is, we look at areas adjacent to the mainshocks before and after they occurred. For the Tennyson foreshocks, it is also possible to look at the time distribution of foreshock occurrence.

The Tennyson Sequence

The 10 February 1990 Tennyson earthquake ($M_L = 5.8$) occurred near the Awatere fault at the northern end of the South Island, New Zealand (Fig. 1). The Awatere fault is part of the Marlborough fault system (Walcott, 1978), which accommodates the transition from the Alpine fault in the south to the Hikurangi subduction zone in the north. The Marlborough faults are predominantly strike slip, as was the mechanism of the Tennyson earthquake determined from long-period body waves (Anderson *et al.*, 1993). The focal depth from the body-wave modeling was 8 km. No detailed study of the Tennyson sequence has yet been undertaken, but portable digital instruments were deployed to record aftershocks, and the data have been incorporated with those from the New Zealand National Seismograph Network in routine processing. The aftershocks form a diffuse zone, slightly elongated in the NE–SW direction, located southeast of the surface trace of the Awatere fault (Fig. 2). It is arguable whether this event occurred as right-lateral slip on the Awatere fault (or a fault subparallel to it), or as left-lateral slip on an unmapped conjugate fault.

Cross-Correlations

The New Zealand National Seismograph Network is now equipped with digital EARSS stations (Gledhill *et al.*, 1991). These instruments currently sample at 50 Hz with antialias filters starting at 15 Hz. All stations are equipped with 1-Hz seismometers, there being a mix of one- and three-component sensors. Sampling is gain-ranged from a 12-bit (plus sign) A/D converter, giving a dynamic range of 120 dB. This large dynamic range allows clean digitization of microseismic noise and on-scale recording of events up to about magnitude 6 by all but the closest stations ($\Delta < \sim 100$ km). Data are recorded on magnetic tape cassettes.

Events for the cross-correlation study were selected by searching the New Zealand catalog in a 1° latitude/longitude region centered on the mainshock epicenter (42.25° S, 172.70° E) for a period of just 1 yr prior to the mainshock, as suitable digital data were only available for this time span. In all, 32 events occurred. The cross-correlations were calculated from the vertical seismograms recorded on the closest EARSS stations. The seismograms were aligned according to hand-picked *P* arrival times and then time shifted by ±5 samples (0.1 sec) to give the best correlation. The cross-correlations were 20 sec long, sufficient to extend from the *P* arrival past the *S* wave train and into the coda. Because New Zealand is an island country, the level of sea-induced microseism is relatively high at periods of 1 to 2 sec. To overcome this, the seismograms were bandpass-filtered between 2 and 15 Hz.

Figure 3 shows the cross-correlation results for station LTZ, 68 km to the southwest of the mainshock. The 2 to 15 Hz bandpass filter (lower left-hand triangle) has served to remove spurious high correlations, such as those

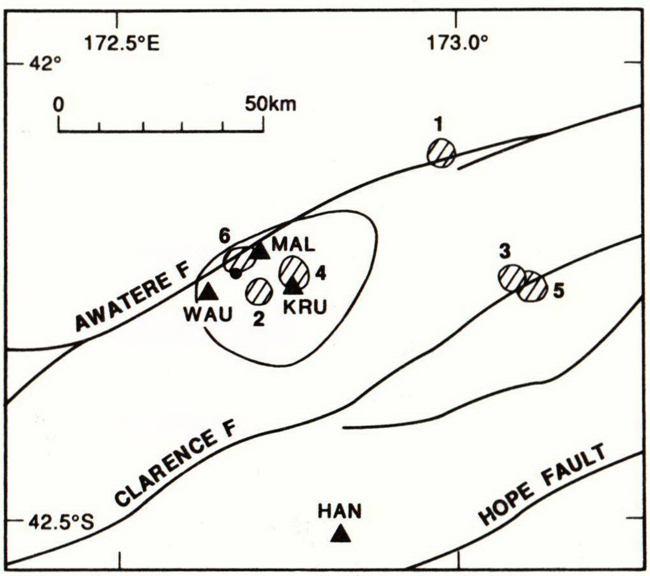

Figure 2. Location of the 1990 Tennyson sequence. The solid dot marks the mainshock, numbers 1 through 6 label the preshock clusters (hatched), and the solid curve marks the extent of the aftershock zone. Active faults (Bowen, 1964) are also shown. Labeled triangles mark the location of temporary seismographs.

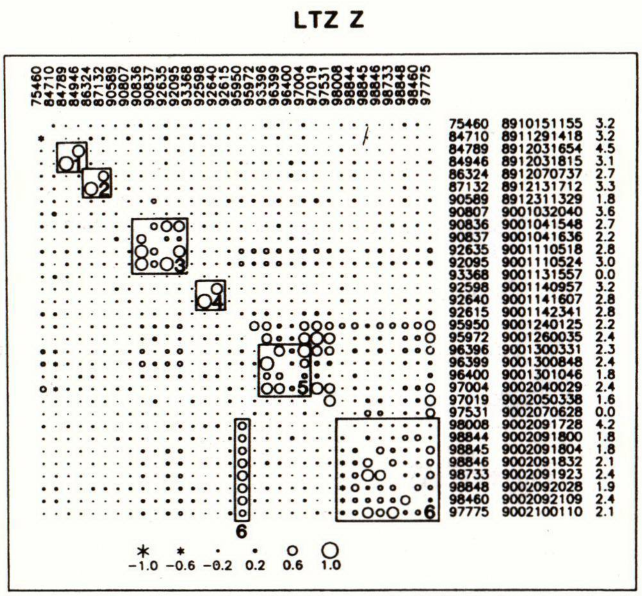

Figure 3. Cross-correlations for the Tennyson preshocks. The key indicates correlation values. Values in the upper triangle are calculated from the raw seismograms, while values in the lower triangle are calculated from data bandpass-filtered between 2 and 15 Hz. Cluster numbers also refer to the locations in Figure 2. Boxes surround groups of events that are considered to be spatially close together on the basis of waveform similarity at all close stations. Each row is labeled with event identification number, date and time string, and M_L.

to the right of cluster 5. The majority of events in the search area are highly correlated with other events, indicating that they occur within 100 to 200 m of each other. The location of each numbered cluster is shown in Figure 2, together with the mainshock location and aftershock zone. The cluster locations were derived by relocating the largest event from each group using *P*-wave arrivals at the three nearest stations (LTZ, KHZ, and THZ) and a restricted focal depth of 10 km (except for cluster 1, which was subcrustal). Where a *P* arrival was not available, the *P* arrival from another nearby station was substituted and the effect of this substitution allowed for by tests with a comparison event. Aftershocks selected from the period when the full network of temporary stations was deployed were relocated by using data from the portables and the three nearest National Network stations. A 2-km eastward adjustment of the clusters and mainshock was then made on the basis of the average mislocation between the relocated aftershocks and their catalog solutions.

All cluster events are shallow except for group 1 events, which have a focal depth of 44 km and are considered to be unrelated to the Tennyson sequence. Clusters 3 and 5 are clearly outside the mainshock rupture zone, but do lie on the surface trace of the Clarence fault. Since these groups are 40 km outside the rupture zone, it is not clear how they are related to the impending mainshock. The occurrence of these events may be coincidental, or this area may be acting as a kind of stress meter in the same way that Sanders and Kanamori (1984) have proposed for the Cahuilla events near Anza, California. Groups 2, 4, and 6 are clearly within the rupture zone and can thus be considered to be preshocks, or in the case of the group 6 events, foreshocks. Of the clusters more numerous than two events (3, 5, and 6), only the immediate foreshocks (cluster 6) have a clear largest event (M_L = 4.2).

To judge the extent to which spatial clustering is a normal feature of background seismicity, we repeated the cross-correlation process for the area 42.6° S to 43.9° S, and 172.0° E to 174.5° E, divided into two overlapping regions (Fig. 1). This area is a band across part of the central South Island, and is tectonically similar to the region of the Tennyson mainshock that is immediately to the north. The first region contained 64 events, 11 of which had filtered cross-correlations greater than 0.5, while for the second region the respective numbers were 147 and 42. In both regions, pairs of highly correlated events were plentiful, but larger groups concentrated in time (such as groups 5 and 6 in Fig. 3) were not present.

Detailed examination of the individual waveforms from the most prominent groups of events in the control areas showed that correlations greater than 0.5 were mostly due to similar *P* waveforms recorded on the LTZ vertical component, followed by very low-amplitude *S* waves and coda. Waveforms on the horizontal components and at another station were, in general, distinctly different. The real spatial clustering in the control areas finally amounted to three event pairs and no clusters more numerous than this. The lack of high correlations is not due to changes in focal mechanism. Such changes vary the *P* to *S* amplitude ratio, but this is a smaller contribution to the cross-correlation than the similarity in each cycle of waveform.

Detailed examination of the clusters in Figure 3 showed that these were genuine spatially coherent groups. Waveforms for the LTZ vertical component for these are shown in Figure 4. The group that shows the poorest correlation is that of the immediate foreshocks (cluster 6). In Figure 4c, these have been ordered according to similarity rather than order of occurrence. The horizontal components at LTZ and a vertical sensor at the other closest station, KHZ, all show more similarity than those shown in Figure 4c, so we are confident of the close

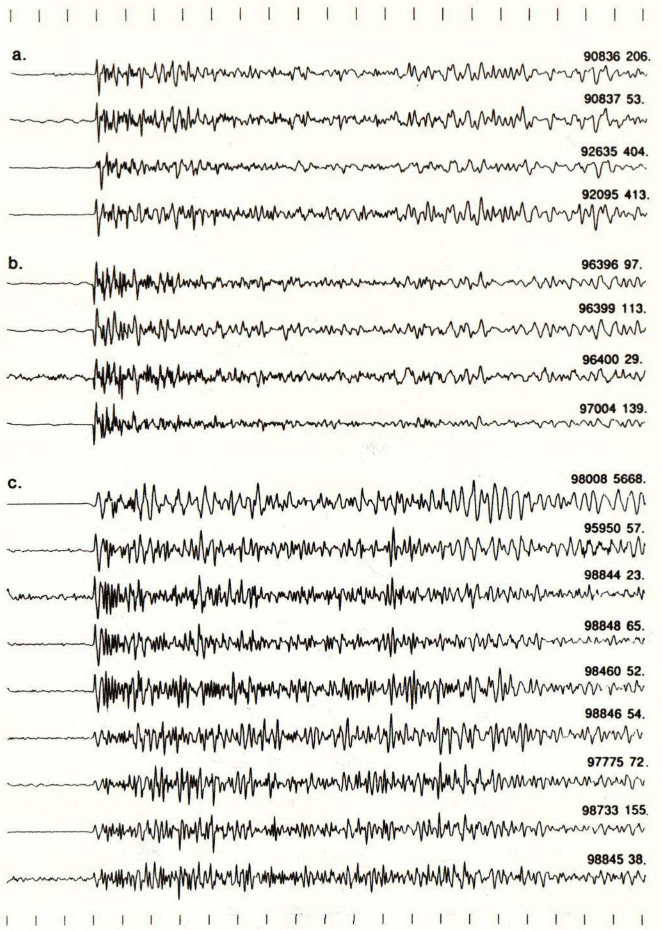

Figure 4. Vertical-component waveforms at station LTZ for each cluster of events shown in Figure 3. (a) Group 3 events, (b) group 5 events, and (c) group 6 events. All traces are normalized to the same amplitude; maximum digital counts for each trace are shown. Vertical bars are at 1-sec intervals.

spatial grouping, although clearly it is not as tight as for clusters 3 and 5. The largest foreshock waveform (98008) is also shown. Its lack of correlation with the other foreshocks is due to its alignment (an earlier *P* pick was made because a long-period low-amplitude arrival was visible above the noise level for this event and not for the others), and its very different frequency content. Its similarity with the other foreshocks is apparent, particularly in the first 6 sec of *P* wave train.

To see whether any aftershocks were spatially close to the preshocks, we cross-correlated all aftershocks that were large enough to be recorded on regional stations with the preshocks. The results for the LTZ vertical component are shown in Figure 5. The lack of any high correlations in the lower left-hand rectangle indicates that no preshocks were similar to the aftershocks. Note though, that there are clusters of similar aftershocks.

Stress Drops

The bonus in finding pairs or clusters of nearly identical events is that sufficiently small events can be deconvolved from larger events to leave the source time function of the larger event. By "sufficiently small," we mean that the duration of the source time function of the small event is much shorter than the larger event. If it is not, the derived source time function will not be a true representation of that of the larger event—it will be shorter by about the width of the small source time function (Frankel and Kanamori, 1983). This method of deriving source time functions has become known as the empirical Green's function technique (Mueller, 1985; Frankel *et al.*, 1986). Here, we have essentially followed the method of Frankel *et al.* (1986). The seismograms from the pair of events being studied were aligned by eye. Where necessary, low-amplitude arrivals from small Green's function events were high-pass filtered with a third-order Butterworth filter, corner frequency 1 Hz, run back and forth over the data to minimize phase shifts. This was not done on the high-amplitude records because of the danger of filtering out some of the larger-event source time functions, and also because of the noncausal nature of the filter. Tests were done on medium-amplitude Green's function events to make sure the filtering did not adversely affect the results. The deconvolution was done by division in the frequency domain, holes in the Green's function spectrum being smoothed out with a two sample width Gaussian filter. Deconvolutions were generally about 1-sec long for the *P* waves and 1 to 2 sec for the *S* waves. *P* waves recorded on vertical sensors were used, while the *S* waves were either deconvolved from vertical seismograms in the case of single-component instruments, or from transverse horizontal seismograms in the case of three-component stations.

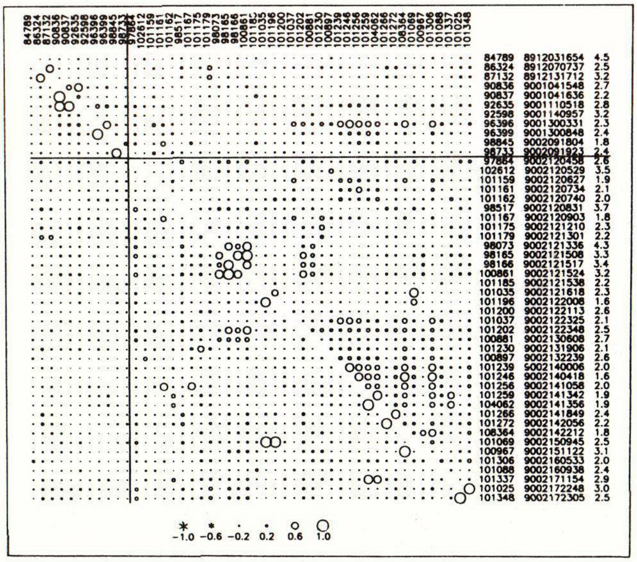

Figure 5. Cross-correlations of Tennyson preshocks with larger aftershocks at station LTZ. The lines separate foreshocks from aftershocks. Only events with at least one cross-correlation value greater than 0.6 are shown for clarity. Details are as for Figure 3.

To date, the empirical Green's function method has usually been applied to local data; i.e., data recorded at close distances so that first arrivals have followed direct, rather than refracted, ray paths. Such data are not routinely available in New Zealand, because the seismograph network is more sparse. However, the ray path is really immaterial—the final seismogram is simply the convolution of the source time function, the path transfer function, and the instrument response. Thus, the deconvolution process should work equally well, as evidenced by the fact that highly correlated events are observed at regional distances. The path transfer function is in theory more complicated, but in the real Earth, where scattering is important, regional and local seismograms do not differ greatly in complexity. High attenuation could remove a lot of the information in the signal, but since most attenuation occurs near the receiver in shallow surface materials (Frankel, 1982), the difference in attenuation between local and regional data is not great.

Figure 6 shows the deconvolved source time functions we have been able to obtain from events in the Tennyson sequence. The consistency between local and regional data is well demonstrated by the aftershocks, where source time functions derived from the regional stations KHZ, LTZ, and MQZ are very similar to the portable data from stations HAN, MAL, WAU, and KRU. The higher-frequency content of the 100-Hz portable data is evident. In some cases, high-frequency deconvolutional noise has been reduced by low-pass filtering the source time function with a bidirectional Butterworth filter of third order (in each pass) and corner frequency of 25 Hz.

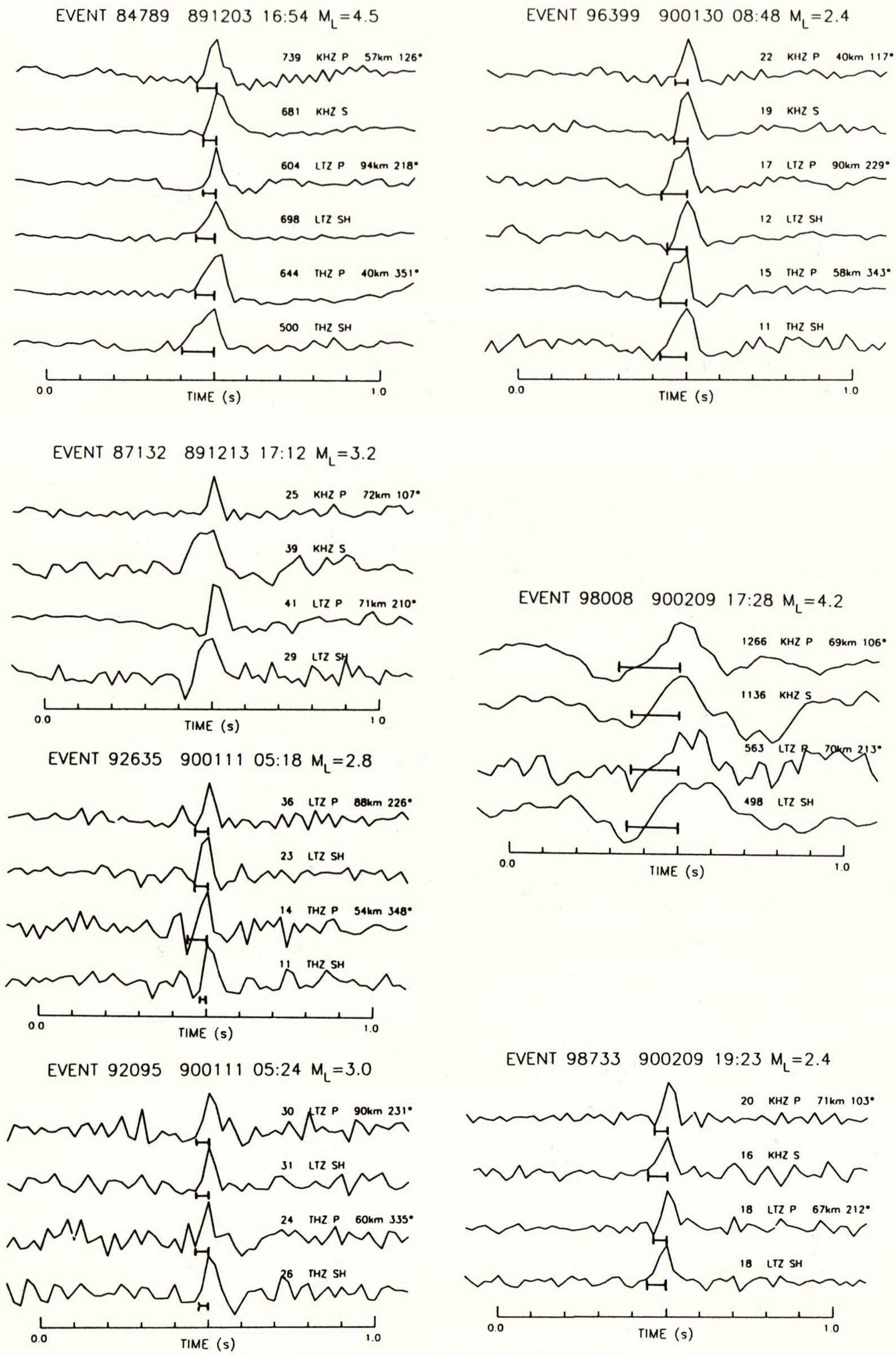

(a)

Figure 6. Source time functions derived by deconvolving empirical Green's functions from events in the Tennyson sequence. The relative amplitude, station, phase, epicentral distance, and azimuth are labeled. *P* and *S* phases were deconvolved from vertical seismograms, while *SH* phases were from the horizontal-component seismograms rotated to the transverse direction. Events are approximately in time order and are labeled with event identification number, origin time, and local magnitude. Aftershocks are from 920212 on.

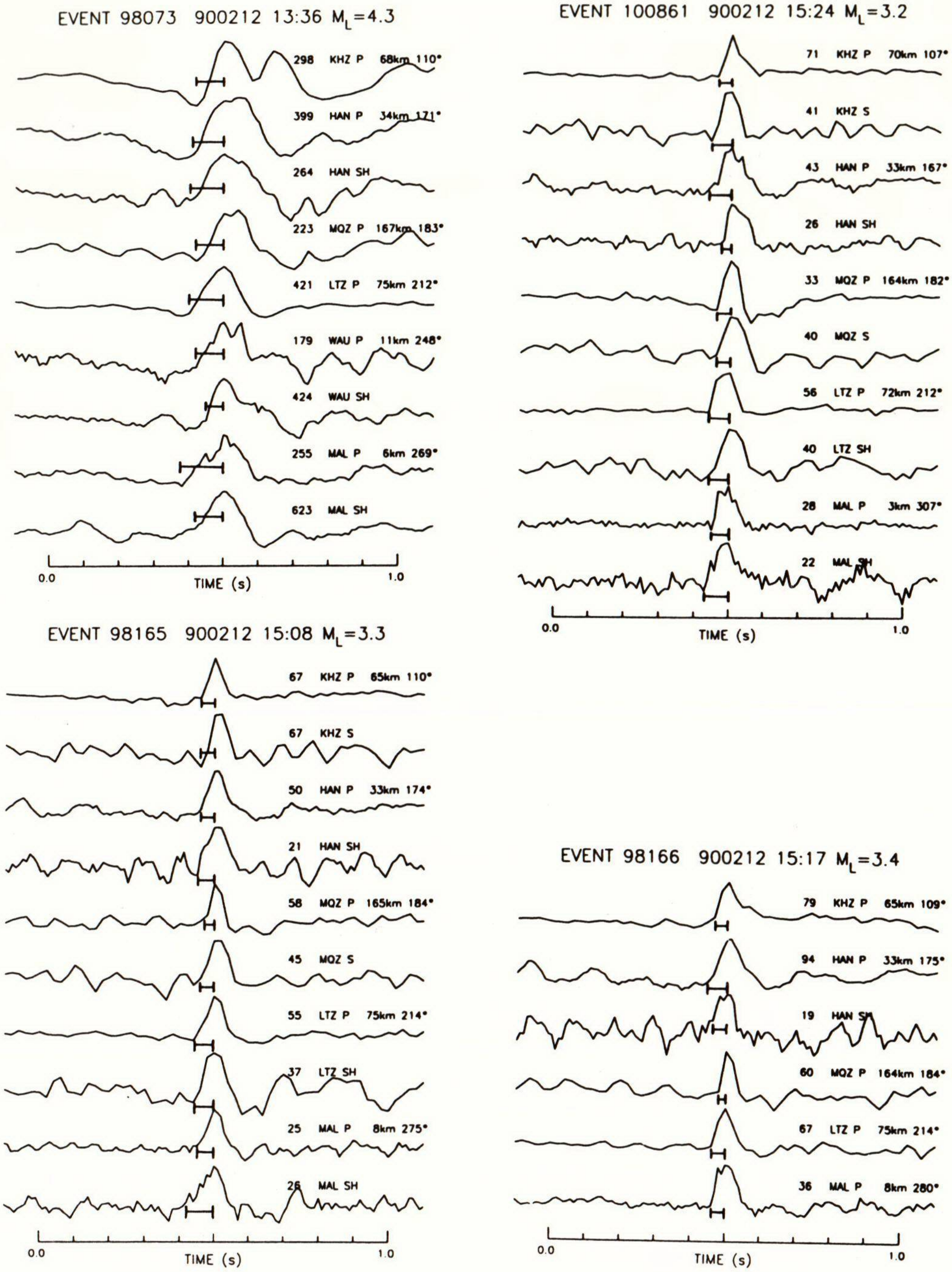

(b)

Figure 6—*Continued*

We had hoped to be able to calculate scalar moments directly for the aftershocks by using the low-frequency spectral level from the portable instrument data, and then deriving moments for the foreshocks by using the relative amplitudes produced in the deconvolution. The lack of any high correlations between the foreshocks and aftershocks precluded this approach, so we have had to fall back on a moment magnitude relation. Since we are only interested in relative values of stress drops for this study, the absolute calibration of moment is not important. The moment magnitude relation that we used was that established for earthquakes near Mammoth Lakes, California, by Archuleta *et al.* (1982),

$$\log M_0 = 1.05\, M_L + 17.75. \qquad (1)$$

To derive fault radius from the source time function pulse rise time ($T_{1/2}$), we must assume a fault rupture model.

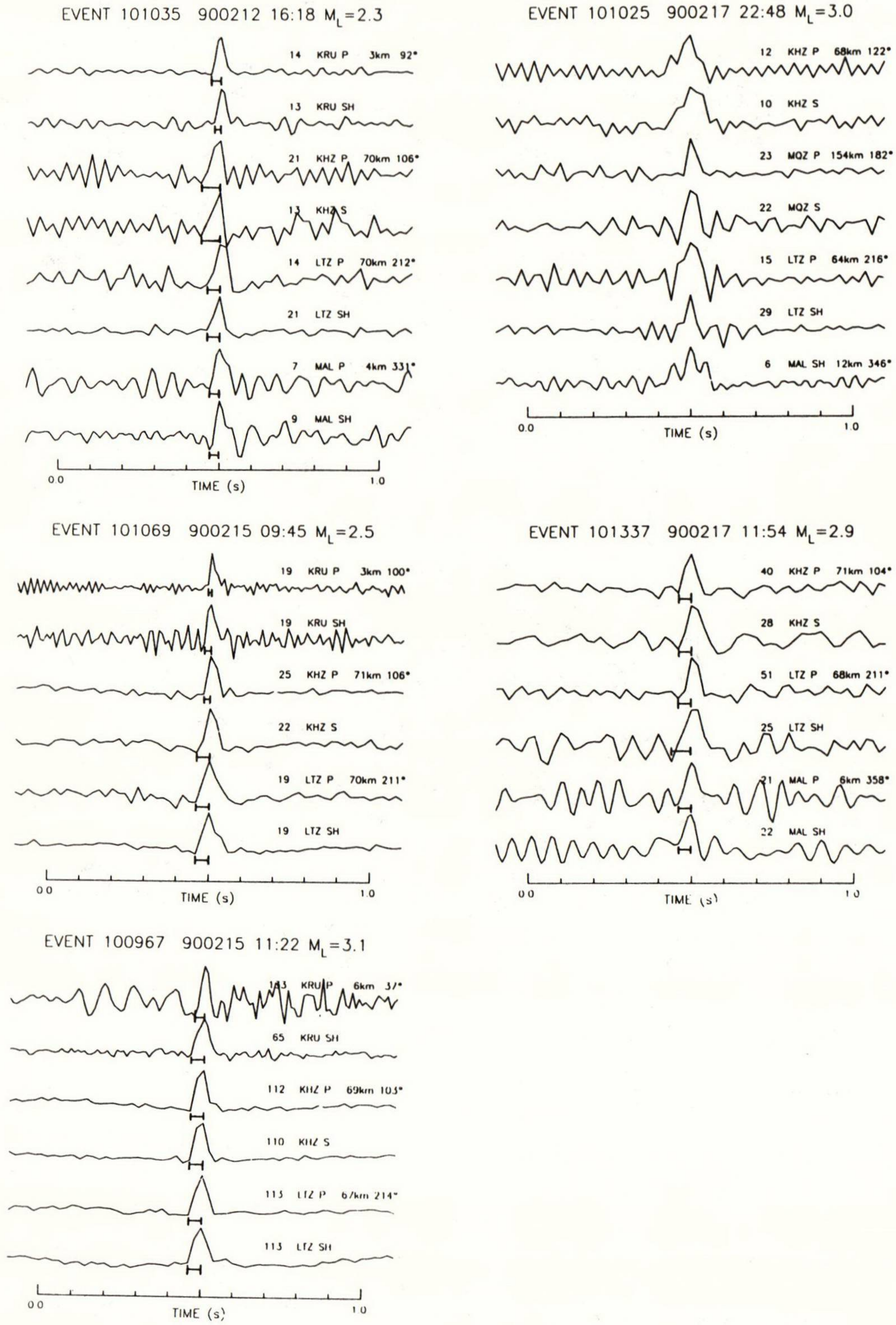

(c)

Figure 6—*Continued*

A commonly used model is that for circular faults (Boatwright, 1980),

$$r = T_{1/2}\, v/(1 - v/c \sin\theta), \quad (2)$$

where v is the rupture velocity, c is the source region P- or S-wave velocity, and θ the angle between the ray take-off direction and the fault normal. A consequence of this model is that $T_{1/2}$ measured from P waves will always be longer than, or equal to, that from S. This is because $T_{1/2}$ is mainly determined by the part of the rupture approaching the receiver, pulse duration being determined by the energy radiated from the receding part of the rupture (Madariaga, 1976). Since a circular rupture model always has a part approaching the receiver, except for the special case where $\theta = 0°$, the ratio of P to S rise times should lie in the range 1.0 to 4.3 as θ varies from 0° to 90°, if source P and S velocities of 6.5 and 3.8 km/sec, respectively, are used. Since the ratio of P to S rise times averages 1.0 for our data, rise times deconvolved from P waves are shorter than from S waves as often as they are longer. This is more indicative of unilateral rupture where, in the case of rupture propagation away from the receiver, the S-wave rise times can be greater than those for P. This observation agrees with that of Frankel *et al.* (1986), who found evidence for unilateral rupture in their study of small earthquakes near Anza, California.

For our study, we do not know the earthquake focal mechanisms or fault-plane orientations with any certainty. We have thus assumed that fault radius is just the product of rise time, $T_{1/2}$, and the assumed rupture velocity of 3.4 km/sec (corresponding to the case $\theta = 0°$ for the circular model). Generally, three regional stations were used over a wide azimuth range that will tend to average out the minor directivity effects that the predominantly unilateral ruptures are producing. Events showing strong directivity were rare and were not included in the stress drop analysis (e.g., event 87132 in Fig. 6).

Once the scalar moment and fault radius had been obtained, we used Brune's (1970) formula,

$$\Delta\sigma = \frac{7}{16}\frac{M_0}{r^3}, \quad (3)$$

to calculate the static stress drop. Parameters for each event are given in Table 1.

The first event in Figure 6 (84789) had a focal depth of 44 km, so we do not consider it to be related to the Tennyson sequence, which occurred in the upper crust. Its rise time is clearly much shorter than events of similar magnitude (i.e., 98873). The stress drop, assuming a rupture velocity of 4 km/sec for that depth, is 1650 bars, with an uncertainty range of 400 to 3400 bars, the uncertainty being estimated from the variability of individual $T_{1/2}$ values. This is a reassuring result, in that we would expect deep events to have higher stress drops than shallow ones as stresses increase with depth. The Green's function event in this case had $M_L = 3.1$. This is larger than we have used for the shallow events, but since this event too should have had a high stress drop, it should not unduly affect the source time function of the larger event. By extrapolating the velocity model of

Table 1
Source Parameters for Events of the Tennyson Sequence

Event ID	Group*	Date	Hr:Min	M_L	M_{LG}†	$T_{1/2}$ (sec)	Radius (km)	Stress Drops (bars) Upper Limit	Stress Drops (bars)	Stress Drops (bars) Lower Limit
84789	1	891203	16:54	4.5	3.1	0.059 ± 0.02	0.20	5723	1653	689
92635	3	900111	05:18	2.8	2.2	0.038 ± 0.02	0.13	956	102	29
92095	3	900111	05:24	3.0	2.2	0.038 ± 0.005	0.13	252	165	114
96399	5	900130	08:48	2.4	1.8	0.063 ± 0.02	0.21	27	9	4
98008	6	900209	17:28	4.2	1.8	0.135 ± 0.031	0.46	147	67	36
98733	6	900209	19:23	2.4	1.8	0.045 ± 0.01	0.15	50	23	13
97781	m.s.	900210	03:27	5.8						
98073	a.s.	900212	13:36	4.3	2.4	0.087 ± 0.02	0.30	696	318	171
98165	a.s.	900212	15:08	3.3	2.4	0.048 ± 0.02	0.16	693	169	65
98166	a.s.	900212	15:17	3.4	2.4	0.040 ± 0.015	0.14	1525	372	143
100861	a.s.	900212	15:24	3.2	2.4	0.051 ± 0.014	0.17	290	111	54
101035	a.s.	900212	16:18	2.3	1.6	0.027 ± 0.02	0.09	4868	85	16
101069	a.s.	900215	09:45	2.5	1.6	0.028 ± 0.02	0.10	5283	123	25
100967	a.s.	900215	11:22	3.1	1.8	0.035 ± 0.006	0.12	475	270	168
101337	a.s.	900217	11:54	2.9	1.9	0.044 ± 0.004	0.15	111	83	64

*Group refers to the event cluster number (Fig. 2) for events prior to the mainshock, m.s. is the mainshock, and a.s. denotes aftershocks.
†M_{LG} is the magnitude of the Green's function event.

Robinson (1986) in a southwesterly direction, we found that this event is part of an intense layer of seismicity in the upper part of the subducting Pacific Plate.

The deconvolved source time functions for the Tennyson sequence show some interesting features (Fig. 6). Event 87132 shows clear directivity at azimuths of 107° and 210°. Since both P waves have narrow pulse widths and fast rise times compared to S, this implies unilateral rupture away from both receivers, i.e., in the north to northwest direction. We did not attempt to estimate the stress drop for this event. Event 92635 shows some evidence for a small subevent, especially in the P waves. Event 98008 has the slowest rise time and broadest source time function of all the events studied. Note the tendency of the source time function pulse to "sink" into the long-period deconvolutional noise. Event 98073 is the largest aftershock we have studied. Again, note the problem of long-period noise. Event 101025 is another example where we may be just resolving a subevent. We did not attempt to use this event for a stress drop determination.

Stress drops for the shallow events are plotted against scalar moment in Figure 7. Since sufficiently small Green's function events were not always available, some Green's function events have magnitudes within 0.6 magnitude units of the larger event. Where the magnitude difference is less than 1.0, we have plotted the data with an asterisk. These data are really an upper limit, because if the Green's function source time function is not a delta function, the deconvolved source time function will be too narrow and the source radius will be underestimated. Uncertainties in stress drop were estimated from the variation in $T_{1/2}$ values where possible, or otherwise by using the maximum sampling interval of 0.02 sec. While one small event has a low stress drop, there is no marked dependence on M_0, a similar result to that obtained by Mori and Frankel (1990).

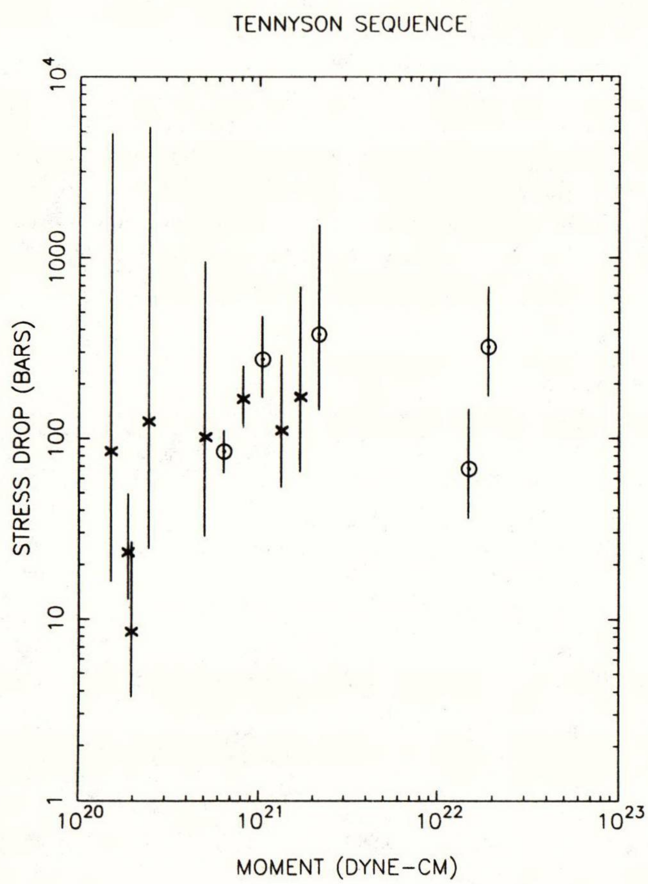

Figure 7. Stress drops of preshocks and aftershocks in the Tennyson sequence plotted as a function of scalar moment. Asterisks denote events with larger Green's functions (see text).

Figure 8 shows the stress drops as a function of time, with the cluster regions noted. The mainshock stress drop should not be directly compared with those of the foreshocks and aftershocks, since it was derived from the rise time of the source time function derived by Anderson *et al.* (1993) from teleseismic data, and by using the teleseismic scalar moment. Although the uncertainties are large, it can be seen that the stress drops for both the events in cluster 5 and the immediate foreshocks (cluster 6) are low compared to the cluster 3 events and the aftershocks. This can be confirmed by comparing the rise times of the largest foreshock and aftershock, which are events of comparable size. The immediate foreshock has slower rise times at all stations than the aftershock.

Rate of Occurrence

Figure 9 shows the time distribution of foreshocks plotted logarithmically from the time of the first and largest foreshock. To see whether this distribution could be distinguished from an aftershock sequence obeying Omori's Law, we looked at the number of events in three equal logarithmic time intervals between the first foreshock and the mainshock. We only have data in two time intervals, giving a value for p in the Omori's Law relation of 0.86, which does not differ remarkably from the usual value of about 1. Extrapolating back to the first time interval (the line in Fig. 9) suggests that there should have been two to three events within that time. A chi-squared test showed that the observed value of 0 is not a significant departure from the expected value of 2.5.

The Weber Sequence

The 19 February 1990 Weber earthquake ($M_L = 5.9$) occurred within the oceanic Pacific Plate being subducted under the North Island, New Zealand (Robinson, 1994, Fig. 10). The mainshock had a normal faulting mechanism (Dziewonski *et al.*, 1991), as is common for this type of event along the Hikurangi Margin (Perin, 1987; Bannister *et al.*, 1989). The aftershock zone covered the depth range 20 to 35 km (Robinson, 1994). This event was followed by a shallow thrust event of magnitude 6.2 in May 1990, and other deep (i.e., 20 to 35 km) events in August 1990 (M_L = 5.6) and March 1992 (M_L = 5.5). This study is focused on activity prior to the February 1990 event.

Cross-Correlations

We followed the same method as for the Tennyson sequence by searching a 1° latitude/longitude region centered on the mainshock epicentre (40.45° S, 176.40° E) for the period from January 1988 until the mainshock. A longer period of recording was available for this region than for the Tennyson area. In all, 553 events shallower than 100 km were selected. Again, cross-correlations were calculated from the vertical seismograms recorded at the nearest EARSS station, PGZ, 22 km to the southwest of the mainshock (Fig. 10). With this number of events it becomes difficult to display the data, but events having a filtered cross-correlation greater than 0.5, 89 in all, are shown in Figure 11. Note that the full cross-correlation matrix is much more sparse than this because of the low correlation events. We have identified four clusters of activity and these are plotted in Figure 10. A close inspection of the waveforms of these events showed that they were tight spatial clusters, not an artifact of similar *P* waves followed by small codas as observed for the Tennyson "control" areas. Cluster 2 is the only one with a clear mainshock (M_L = 4.9). Focal depths indicated that all four clusters were located within the subducting Pacific Plate.

In Figure 10 we have also plotted the location of one immediate foreshock (M_L = 3.6), the mainshock, and the aftershock zone as relocated by Robinson (1994). The spatial clusters are all located well outside the rupture zone. Of 37 events in the 6 weeks prior to the mainshock relocated by Robinson (1994), only four fell within the aftershock zone, and one of these occurred 11 hr before the mainshock. None of these four events feature in Figure 11 because all had maximum cross-correlations less than 0.5, which implies that they did not form a close spatial cluster.

To see how common clusters such as 1 through 4 in Figure 10 are in this region, we repeated the cross-correlation exercise for all events in the area 40.9° S to 41.5° S, and 175.6° E to 176.4° E, for the period January 1990

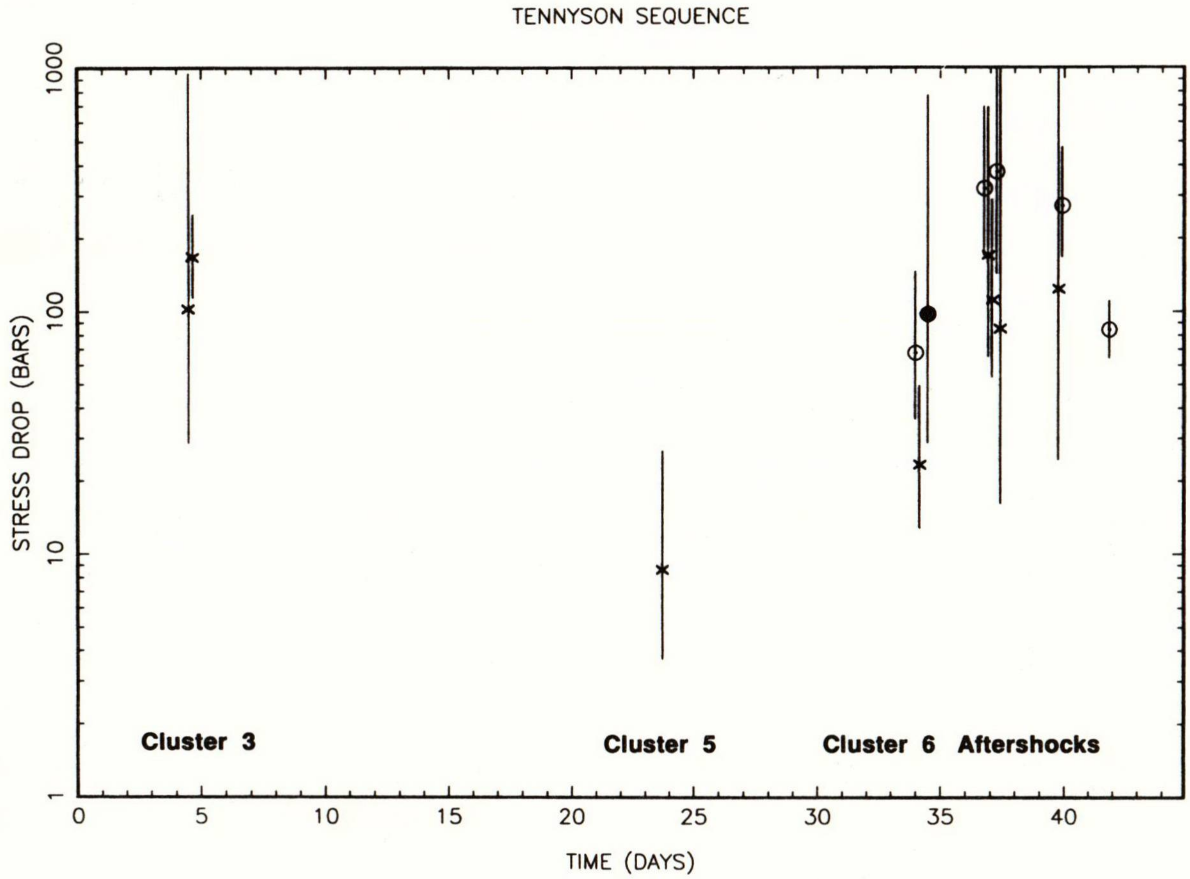

Figure 8. Stress drops of preshocks and aftershocks in the Tennyson sequence as a function of time. Numbers refer to the cluster regions shown in Figure 2. The solid circle marks the mainshock, and asterisks denote events with larger Green's functions (see text).

through March 1992. This region was selected because it is midway between the Weber area and Cape Palliser, where an $M_L = 5.3$ event occurred in October 1990, and is also close to station PGZ. Of the 299 events selected, at least eight (in September 1991) formed a close spatial cluster, comprising a magnitude 4.3 event followed by aftershocks. This is shown as cluster 5 in Figure 10.

Since our clusters 1 through 4 are well removed from the mainshock rupture zone in space and time, we contend that they are not related to the impending mainshock. This contention is supported by the fact that we were able to find cluster 5 in a region further from, and after, the February 1990 mainshock. Another $M_L = 5.5$ event did occur adjacent to, and northeast of, the rupture zone in March 1992, but that is 100 km from cluster 5. Furthermore, Smith and Webb (1986) found that earthquake swarms do occur along the Hikurangi Margin. Whether all such swarms show spatial clustering is not known, but a swarm studied in the Taupo volcanic zone did (Sherburn, 1993).

In an attempt to get stress drops for the Weber foreshocks, we cross-correlated ten events from near the rupture zone, including three of those relocated within the aftershock zone by Robinson (1994), with all of the aftershocks. No events had sufficiently high correlations to use as an empirical Green's function for a deconvolution, so no stress drops could be obtained.

Discussion

The results from our cross-correlation analysis are mixed. The clusters of activity preceding the Tennyson event are distinguishable from background seismicity by being more numerous than doublets. We consider doublets to be a part of the normal activity in that continental strike-slip environment. The doublets near the Tennyson mainshock (clusters 2 and 4) are probably related to the mainshock, but that would not have been obvious at the time. The more abundant precursory clusters 3 and 5 occurred in the 38 days preceding the mainshock, but were 40 km outside the final rupture zone. Only the immediate foreshocks consisted of a cluster of more than two events and occurred within the aftershock zone. This group also had one event clearly larger than the others, so it may have been difficult to distinguish at the time from a small mainshock followed by aftershocks.

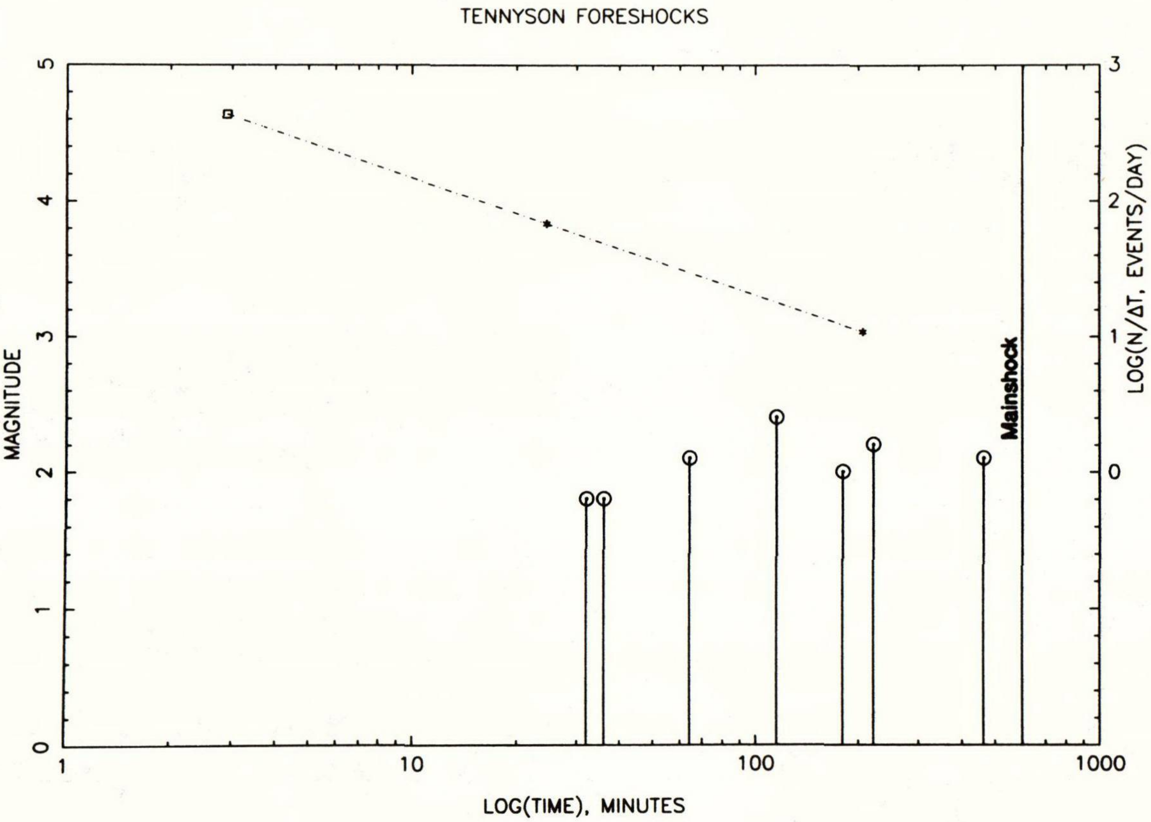

Figure 9. Logarithmic time distribution from the first foreshock to the mainshock (vertical bar) in the Tennyson sequence. Equal logarithmic time intervals used in the Omori's Law analysis are shown by vertical bars. The asterisks mark rate of activity values (on the right hand axis), and are extrapolated back to the first time interval to calculate the expected value of activity of two to three events.

Deciding whether the cluster activity prior to and near to, but outside, rupture zones is related to the following mainshock is problematical. Here we have attempted to use "control" areas to see how common such clustered activity is, but that still gives an incomplete picture. The task of examining the entire New Zealand region for the total period of digital recording to date is well beyond our current resources, and even then may not produce a definitive answer because of the limited data set and a sufficient number of large events to relate clusters to. Evison (1982), in his precursory swarm hypothesis, generally requires precursory swarms and mainshocks to have overlapping regions. If we applied such a criterion here, we could only regard the immediate foreshocks of the Tennyson sequence as precursory. However, as mentioned earlier, clusters 3 and 5 may be acting as a kind of stress meter, such as proposed by Sanders and Kanamori (1984). The seismicity prior to the Tennyson mainshock has the additional feature of alternating between two distinct regions. Again, it is difficult to judge the significance of this.

For the Weber sequence, we consider the observed clustering to be part of normal background seismicity at a subduction zone margin because it all occurred well outside the final rupture zone, covering time periods greater than 1 yr before (and after) the mainshock. Cluster 1 of the Tennyson sequence also falls into this category.

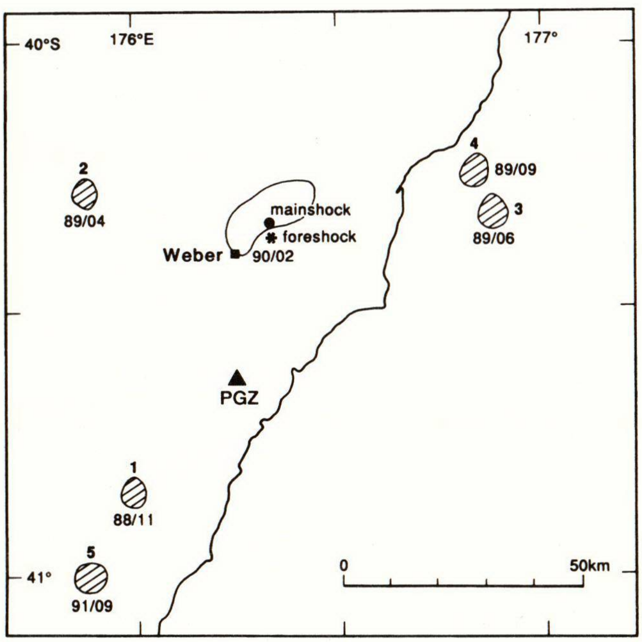

Figure 10. Location of the February 1990 Weber sequence. The solid circle marks the mainshock, the asterisk the immediate foreshock, and the curve outlines the aftershock zone. Numbered circles denote the location of cluster activity referred to in the text and in Figure 11. Each is labeled with the year and month of occurrence. EARSS station PGZ is marked with a solid triangle.

Pechmann and Thorbjarnardottir (1990) have interpreted precursory clustering in terms of the asperity model of Kanamori (1981). The lack of such clustering can be explained qualitatively by a fault that is homogeneous in terms of strength, so that no particular parts of it fail prior to the mainshock. Is such a homogeneous model appropriate for the upper part of the subducting oceanic crust that is undergoing normal faulting as part of the bending process (e.g., Bannister *et al.*, 1989)? We do not think so, because both swarm activity and spatial clustering are present throughout the region studied, and such features of seismicity have been cited as indicating heterogeneity (Sykes, 1970; Pechmann and Thorbjarnardottir, 1990). Again, the cross-correlation technique would need to be applied to the whole margin before we could be more confident of what the relationship between the clusters and the large events is.

It is worth noting that all of the spatial clusters identified in this study were also clusters in time, except for one Tennyson foreshock. This was also true for the preshocks observed by Pechmann and Kanamori (1982). Note that this is not the case for aftershocks, but only because the higher rate of activity in the selected region means clusters become intermingled in time. However, Cole *et al.* (1992) have observed identical earthquakes repeating over periods of years. Spatial clusters that are close in time may be events on adjacent segments of a fault, while those years apart are rupturing the same fault segment.

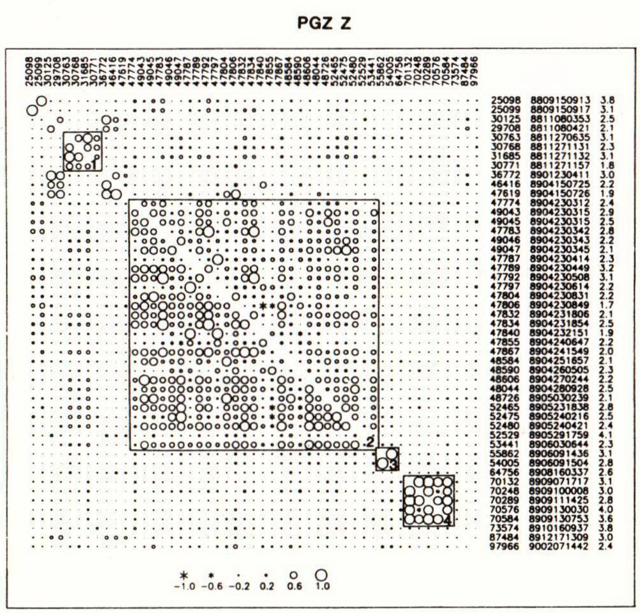

Figure 11. Cross-correlations for the Weber preshocks. Details are the same as for Figure 3, except that the cluster numbers refer to locations given in Figure 10, and only events with a cross-correlation greater than 0.6 are included.

Our results show that events during the 15 days prior to the Tennyson mainshock had lower stress drops than either earlier events or aftershocks. This is also true of an event in cluster 5 that was outside the final rupture zone. Foreshocks should have high stress drops, reflecting the high crustal stress levels before an incipient main event (Kanamori, 1981). This is what Mori and Frankel (1990) found for a North Palm Springs, California, preshock. However, Bakun and McEvilly (1979) found that one 1966 Parkfield foreshock was clearly of lower frequency than the aftershocks and other normal events recorded at the same station. Another foreshock had a similar frequency content to the normal events. A possible explanation for lower stress levels before major events is preseismic creep. An earthquake instability model invoking strain weakening before a mainshock, such as that proposed by Stuart *et al.* (1985), would be consistent with low stress drop earthquakes related to the creep process. In our case, we have the added complexity of one low stress drop event occurring 40 km outside the rupture zone. We can only speculate that if this was due to preseismic creep on the neighboring fault, then that creep process must have stopped, perhaps because of the nearby mainshock. An alternative explanation is that the stress drop is inaccurate because the event consisted of two subevents that could not be resolved.

Motoya and Abe (1985) found similarity between foreshocks and, separately, between aftershocks for the 1981 Eniwa, Hokkaido, earthquake. Only one aftershock was highly correlated with the foreshocks. This is consistent with the complete lack of correlation between foreshocks and aftershocks for both of the sequences we have studied, where the foreshocks occurred within the location uncertainty of the epicenters, or rupture initiation points (Figs. 2 and 10). The lack of correlation with the aftershocks thus suggests that the foreshocks occurred near to the rupture initiation point, where coseismic stress release was complete.

Oppenheimer *et al.* (1990) have found, for three Calaveras fault events, that background seismicity and aftershocks occur in the same general locations, while areas of maximum slip are largely aseismic. It is not possible to identify foreshock locations from their analysis, but our results would suggest that they should occur within the aseismic region. Note though, that with the waveform cross-correlation analysis, we are dealing with differences in location of hundreds of meters, while their discussion relates to a kilometer scale.

Conclusions

1. Tennyson foreshocks had very similar waveforms, indicating that they occurred in the same location (within a few 100 m) inside the final aftershock zone. Two other clusters of activity occurred in the 38 days before the mainshock in one location, 40 km outside the aftershock zone. Their relationship to the following mainshock is not clear.
2. Stress drops of three events before the Tennyson mainshock were lower than for earlier events and aftershocks.
3. Deconvolved source time functions for Tennyson events fit a unilateral rupture model better than a circular source model.
4. There were only four Weber foreshocks, all dissimilar, and also different from the aftershocks. Spatial clustering prior to the mainshock was observed, but well outside the aftershock zone. This is considered to be part of the normal background activity within the subducting oceanic crust along the Hikurangi Margin.
5. In neither of the two sequences studied were foreshocks highly correlated with aftershocks, suggesting that they occurred in regions where coseismic slip relieved all accumulated shear stress.
6. A stress drop of 1650 bars was obtained for a 44-km-deep $M_L = 4.5$ earthquake located in the upper part of the subducting oceanic crust near the southern end of the Hikurangi Margin.

Acknowledgments

This study was partly funded by grant 91/37 from the New Zealand Earthquake and War Damage Commission. Art Frankel kindly provided the original version of the deconvolution program, Russell Robinson calculated the location of the Weber event foreshock relative to the mainshock and aftershocks. Staff from the then Geophysics Division of DSIR and from Victoria University of Wellington are gratefully acknowledged for their participation in collecting the aftershock data. Russell Robinson, Stephen Bannister, Geoff Gregory, and two anonymous referees made helpful comments on the manuscript.

References

Anderson, H. J., T. H. Webb, and J. Jackson (1993). Focal mechanisms of large earthquakes in the South Island, New Zealand; implications for the accommodation of Pacific-Australia plate motion, *Geophys. J. Int.* **115**, 1032–1054.

Archuleta, R. J., E. Cranswick, C. Mueller, and P. Spudich (1982). Source parameters of the 1980 Mammoth Lakes, California earthquake sequence, *J. Geophys. Res.* **87**, 595–607.

Bakun, W. H. and T. V. McEvilly (1979). Are foreshocks distinctive? Evidence from the 1966 Parkfield and the 1975 Oroville, California, sequences, *Bull. Seism. Soc. Am.* **69**, 1027–1038.

Bannister, S. C., B. J. Perin, and T. H. Webb (1989). Normal faulting through subducted oceanic crust: the 19 July 1985 earthquake of Hawke's Bay, New Zealand, *Tectonophysics* **162**, 303–313.

Boatwright, J. (1980). A spectral theory for circular seismic sources; simple estimates of source dimension, dynamic stress drop, and radiated seismic energy, *Bull. Seism. Soc. Am.* **70**, 1–27.

Bowen, F. E. (1964). Sheet 15, Buller, Geological Map of New Zealand 1:250,000, Department of Scientific and Industrial Research, Wellington, New Zealand.

Brune, J. N. (1970). Tectonic stress and the spectra of seismic shear waves from earthquakes, *J. Geophys. Res.* **75**, 4997–5009.

Cole, A. T., W. L. Ellsworth, and G. C. Beroza (1992). Determining earthquake kinship from waveform catalogs, *EOS* **73**, 344.

Dziewonski, A. M., G. Ekstrom, J. H. Woodhouse, and G. Zwart (1991). Centroid moment tensor solutions for January–March, 1990, *Phys. Earth Planet. Interiors* **65**, 197–206.

Evison, F. F. (1982). Generalised precursory swarm hypothesis, *J. Phys. Earth* **30**, 155–170.

Frankel, A. (1982). Effects of attenuation and site response on the spectra of microearthquakes in the northeastern Caribbean, *Bull. Seism. Soc. Am.* **72**, 1379–1402.

Frankel, A. (1984). Source parameters of two $M_L = 5$ earthquakes near Anza, California, and a comparison with an Imperial Valley aftershock, *Bull. Seism. Soc. Am.* **74**, 1509–1527.

Frankel, A., J. Fletcher, F. Vernon, L. Haar, J. Berger, T. Hanks, and J. Brune (1986). Rupture characteristics and tomographic source imaging of $M_L = 3$ earthquakes near Anza, southern California, *J. Geophys. Res.* **91**, 12633–12650.

Frankel, A. and H. Kanamori (1983). Determination of rupture duration and stress drop from earthquakes in southern California, *Bull. Seism. Soc. Am.* **73**, 1527–1551.

Geller, R. J. and C. S. Mueller (1980). Four similar earthquakes in central California, *Geophys. Res. Lett.* **7**, 821–824.

Gledhill, K. R., M. J. Randall, and M. P. Chadwick (1991). The EARSS digital siesmograph: system description and field trials, *Bull. Seism. Soc. Am.* **81**, 1380–1390.

Ishida, M. and H. Kanamori (1978). The foreshock activity of the 1971 San Fernando earthquake, California, *Bull. Seism. Soc. Am.* **68**, 1265–1279.

Ishida, M. and H. Kanamori (1980). Temporal variation of seismicity and spectrum of small earthquakes preceding the 1952 Kern County, California, earthquake, *Bull. Seism. Soc. Am.* **70**, 509–527.

Kanamori, H. (1981). The nature of seismicity patterns before large earthquakes, in *Earthquake Prediction: An International Review, Maurice Ewing Series 4*, D. W. Simpson and P. G. Richards (Editors), American Geophysical Union, Washington, D.C., 1–19.

Madariaga, R. (1976). Dynamics of an expanding circular fault, *Bull. Seism. Soc. Am.* **66**, 639–666.

Mori, J. and A. Frankel (1990). Source parameters for small events associated with the 1986 North Palm Springs, California, earthquake determined using empirical Green functions, *Bull. Seism. Soc. Am.* **80**, 278–295.

Motoya, Y. (1990). A practical approach to identifying foreshocks, *EOS* **71**, 908.

Motoya, Y. and K. Abe (1985). Waveform similarity among foreshocks and aftershocks of the October 18, 1981, Eniwa, Hokkaido, earthquake, *Earthquake Predict. Res.* **3**, 627–636.

Mueller, C. S. (1985). Source pulse enhancement by deconvolution of an empirical Green's function, *Geophys. Res. Lett.* **22**, 33–36.

Oppenheimer, D. H., W. H. Bakun, and A. G. Lindh (1990). Slip partitioning of the Calaveras Fault, California, and prospects for future earthquakes, *J. Geophys. Res.* **95**, 8483–8498.

Pechmann, J. C. and H. Kanamori (1982). Waveforms and spectra of preshocks and aftershocks of the 1979 Imperial Valley, California, earthquake: evidence for fault heterogeneity? *J. Geophys. Res.* **87**, 10579–10597.

Pechmann, J. C. and B. S. Thorbjarnardottir (1990). Waveform analysis of two preshock-mainshock-aftershock sequences in Utah, *Bull. Seism. Soc. Am.* **80**, 519–550.

Perin, B. J. (1987). Body-wave modelling of earthquakes, Hikurangi Margin, New Zealand, *Master's Thesis*, Victoria University of Wellington, New Zealand, 151 pp.

Robinson, R. (1986). Seismicity, structure and tectonics of the Wellington region, New Zealand, *Geophys. J. R. Astr. Soc.* **87**, 379–409.

Robinson, R. (1994). The Weber, New Zealand, earthquake sequence of 1990–1992, *J. Geophys. Res.* **99**, 9663–9679.

Sanders, C. O. and H. Kanamori (1984). A seismotectonic analysis of the Anza seismic gap, San Jacinto Fault Zone, southern California, *J. Geophys. Res.* **89**, 5873–5890.

Sherburn, S. (1993). The 1987 January Tokaanu earthquake sequence, New Zealand, *N. Z. J. Geol. Geophys.* **36**, 61–68.

Smith, E. G. C. (1981). Foreshocks of shallow New Zealand earthquakes, *N. Z. J. Geol. Geophys.* **24**, 579–584.

Smith, E. G. C. and T. H. Webb (1986). The seismicity and related deformation of the Central Volcanic Region, North Island, New Zealand, in Late Cenozoic Volcanism in New Zealand, in *Royal Society of N. Z. Bulletin 23*, I. E. M. Smith (Editor), Royal Society of New Zealand, Wellington, New Zealand, 112–133.

Stuart, W. D., R. J. Archuleta, and A. G. Lindh (1985). Forecast model for moderate earthquakes near Parkfield, California, *J. Geophys. Res.* **90**, 592–604.

Sykes, L. R. (1970). Earthquake swarms and seafloor spreading, *J. Geophys. Res.* **75**, 6598–6611.

Thorbjarnardottir, B. S. and J. C. Pechmann (1987). Constraints on relative earthquake locations from cross-correlation of waveforms, *Bull. Seism. Soc. Am.* **77**, 1626–1634.

Tsujiura, M. (1977). Spectral features of foreshocks, *Bull. Earthquake Res. Inst.* **52**, 357–371.

Walcott, R. I. (1978). Present tectonics and late Cenozoic evolution of New Zealand, *Geophys. J. R. Astr. Soc.* **52**, 137–164.

Institute of Geological and Nuclear Sciences
Wellington
New Zealand

Manuscript received 30 November 1992.

Institute of
GEOLOGICAL & NUCLEAR SCIENCES
Limited

Foreshocks of the 1990 Tennyson and Weber earthquakes - could they have been recognised?

Terry H. Webb

Contract Report No. 1992/58

Institute of
GEOLOGICAL
& NUCLEAR
SCIENCES
Limited

FORESHOCKS OF THE 1990 TENNYSON AND WEBER EARTHQUAKES - COULD THEY HAVE BEEN RECOGNISED?

CONTRACT REPORT NO. 1992/58

Prepared for

The Earthquake and War Damage Commission

as Project 91/37

Terry H. Webb

July 1992

32 Salamanca Road, PO Box 1320, Wellington, New Zealand, Telephone: +64-4-473 8208, Facsimile: +64-4-471 0977

A Crown Research Institute

CONTENTS

Summary....3

1.0 Introduction....3

2.0 The Tennyson Sequence....4

2.1 Waveform Similarity....4

2.2 Stress Drops....5

3.0 The Weber Sequence....5

4.0 Conclusions....6

References....7

Figure 1. The Tennyson sequence. Numbered shaded regions show the location of precursory clusters. Note that cluster 1 is deep and not related to the sequence. The curve encircling clusters 2, 4, and 6 outlines the aftershock zone. The solid dot marks the mainshock. 8

Figure 2. Stress drops of preshocks and aftershocks as a function of time. The cluster region locations are shown in Figure 1. The stress drop of the mainshock in marked by the solid circle and is only approximate. 9

Figure 3. Location of the 1990 February Weber sequence. The solid circle marks the mainshock, the asterisk the immediate foreshock, and the curve outlines the aftershock zone. Numbered circles denote the location of cluster activity, each being labelled with the year and month of occurrence. EARSS station PGZ is marked with a solid triangle. 10

FORESHOCKS OF THE 1990 TENNYSON AND WEBER EARTHQUAKES - COULD THEY HAVE BEEN RECOGNISED?

Terry H. Webb

SUMMARY

The foreshocks of the M_L= 5.8 Tennyson earthquake had very similar waveforms indicating that they occurred in the same location (within a few 100 metres) inside the final aftershock zone. Two other clusters of activity occurred in the 38 days before the mainshock in one location 40 km outside the aftershock zone. These separate clusters were apparently related to the following mainshock, but the actual physical relationship is not clear. This study shows that such clustering activity is unusual in this area, but more investigation is needed before we can be confident that it is always related to an impending mainshock. Stress drops of three events before the Tennyson mainshock were lower than for earlier events and aftershocks. This is an unexpected result that can possibly be explained by pre-seismic creep occurring before the mainshock. A major limitation in the stress drop analysis was the low 50 Hz sampling rate used by the National Network seismograph stations. There were only 4 Weber foreshocks, and they did not have similar waveforms. Spatial clustering of background seismicity prior to the Weber mainshock was observed, but it was well outside the aftershock zone. This is considered to be part of the normal background activity within the subducting oceanic crust along the Hikurangi Margin.

1.0 INTRODUCTION

The work described in this report has been written up for publication in the Bulletin of the Seismological Society of America, and at the time of writing was undergoing internal review prior to submission to the journal. The following is an overview of the research carried out in the project : the reader should refer to the BSSA paper for details of the analysis and results.

The aim of this study was to look in detail at the foreshocks of the 1990 February Tennyson and Weber earthquakes to see if they were different in any way from other "normal" earthquakes in the area, or from aftershocks. In particular, the similarity of the digital seismograms of the various events has been examined. Some seismologists (e.g. Motoya and Abe, 1985; Pechmann and Kanamori, 1982) have found that foreshocks are all very similar to each other, indicating that they occur at the same location within 100 to 200 m, perhaps at one last localised strong point on the fault. This location accuracy is much better than we can achieve with traditional earthquake location methods using phase arrivals at distant stations, which have uncertainties of 5 to 10 km.

Using advanced deconvolution techniques we can also calculate the stress in the earth released by the earthquake (the stress drop), if we have two events with similar waveforms, but of different size. One might expect foreshocks to have higher than normal stress drops because they occur where a large earthquake is about to happen.

2.0 THE TENNYSON SEQUENCE

2.1 Waveform Similarity

The earthquakes in the two months before the Tennyson mainshock clustered into five distinct groups (see Figure 1). Two of these groups were identical pairs of events that occurred within the final rupture zone of the earthquake. Two further groups, each of four events, occurred at almost the same location near the Clarence Fault, 40 km to the east of the rupture zone. The fifth cluster of immediate foreshocks were moderately well-correlated and occurred within the aftershock zone, very near to where the mainshock rupture started.

It was not clear just how the clustered activity was related to the impending mainshock. To get a better idea of how common such activity is, three control areas across the central South Island were searched. In two of these areas some pairs of similar events were found, but no clusters. However, in the third area there were two clusters of activity. This suggested that such clusters are relatively common and that the clusters 40 km from the Tennyson mainshock were coincidental. Furthermore, it became clear that the immediate foreshocks of the Tennyson event could not be distinguished from such clusters. This was the conclusion of the March progress report.

Since March, a more careful examination of the clusters in the third control area has brought to light an interesting fact. The two clusters of activity that occurred there were located within 29 km and 42 km of the magnitude 5.5 earthquake that occurred on 1992 March 30, west of Lake Coleridge. Since this work was by then in an advanced stage of preparation for publication, the results from the third control area have not been included. Those results may be used in a future study of the Coleridge and 1991 Hawk's Crag earthquakes. In light of the Coleridge earthquake, the clusters 40 km from the Tennyson mainshock no longer appear to be coincidental, but it is still not clear how they are physically related to that mainshock. Sanders and Kanamori (1984) noted that swarm activity near the San Jacinto fault in California has, in the past, occurred before large earthquakes. The Chinese have also talked of "sensitive areas" that become active before major events.

2.2 Stress Drops

Calculating stress drops is a tricky business because it is very difficult to remove the effects of seismic wave propagation through the earth to get the true signal that left the earthquake source. This project has examined some 5000 earthquakes, and it has only been possible to calculate stress drops for 14. A more exhaustive analysis using bigger computing facilities may allow more aftershock stress drops to be obtained. The number is limited firstly by the need to find identical event pairs, and secondly by events being of sufficiently long duration to measure the source process with sufficient accuracy. This accuracy is limited by the low 50 Hz digital sampling rate used by the New Zealand seismograph stations. Most overseas networks use at least 100 Hz sampling which greatly improves the data quality.

The stress drop results show that three events before the mainshock had lower stress drops than earlier preshocks and later aftershocks (see Figure 2). This is the opposite result to what was expected. There is one report in the literature of a similar result for a Parkfield, California foreshock. One speculative interpretation of the low stress drop values is that, just before the mainshock, the fault begins to slip slowly. This phenomenon is known as pre-seismic creep, and the small earthquakes associated with it could be expected to have low stress drops.

3.0 THE WEBER SEQUENCE

Four clusters of highly correlated earthquakes occurred before the 1990 February Weber mainshock (see Figure 3). However, they ranged in distance from 40 km to 55 km from the final rupture zone, and occurred between 5 and 15 months before the mainshock. Because of the separation in distance and time, this activity was apparently not directly related to the mainshock. Analysis of a control area to the south found a cluster 80 km from the rupture zone 19 months after the first Weber event. This was prior to the 1992 March Weber earthquake, but 100 km from it. It seems that such clusters of activity are part of the normal background seismicity along the Hikurangi subduction zone.

Four earthquakes occurred near the final Weber rupture zone in the month before the mainshock. These can be considered to be foreshocks. They were not at all similar to each other, so did not occur in the same place, and could not have been distinguished from normal background seismicity at the time. It was not possible to find any aftershocks similar to the foreshocks, which meant that no stress drops could be determined.

4.0 CONCLUSIONS

The Tennyson foreshocks had very similar waveforms, indicating that they occurred in the same location (within a few 100 metres) inside the final aftershock zone. Two other clusters of activity occurred in the 38 days before the mainshock in one location 40 km outside the aftershock zone. These separate clusters were apparently related to the following mainshock, but the actual physical relationship is not clear. Stress drops of three events before the Tennyson mainshock were lower than for earlier events and aftershocks. Two further clusters of activity were found near the 1992 March Coleridge earthquake. They may be analysed in detail in a future project.

There were only 4 Weber foreshocks, all dissimilar, and also different from the aftershocks. Spatial clustering prior to the mainshock was observed, but it was all well outside the aftershock zone. This is considered to be part of the normal background activity within the subducting oceanic crust along the Hikurangi Margin.

Both sequences were subject to the problem of deciding whether nearby clusters of activity are related to the impending mainshocks. An attempt was made to resolve this problem by looking at control areas. However, the problem can really only be resolved by examining in detail the seismicity of the whole country. This is a large undertaking, and may not yield an unambiguous answer because both spatial clusters and moderate magnitude earthquakes are relatively common. Since this project was formulated there have been five other moderate magnitude earthquake sequences. All are worthy of a similar investigation as we have given the Tennyson and first Weber events.

Despite the lack of definitive results, careful analysis of stress drops still holds the most promise for learning about the seismic source. A spin-off of this analysis is that the way in which earthquakes rupture can be studied, i.e. does rupture begin at a point and spread out in a circle over the fault plane, or does it head off in one predominant direction? The results of this study support the latter interpretation. However, the New Zealand National Network data is of limited use for such studies because of the low digital sampling rate of 50 Hz being used. The introduction of 100 Hz sampling throughout the country would be extremely helpful for studies such as this.

REFERENCES

Motoya, Y. and K. Abe (1985). Waveform similarity among foreshocks and aftershocks of the October 18, 1981, Eniwa, Hokkaido, earthquake, *Earthq. Predict. Res. 3*, 627-636.

Pechmann, J.C. and H. Kanamori (1982). Waveforms and spectra of preshocks and aftershocks of the 1979 Imperial Valley, California, earthquake: Evidence for fault heterogeneity?, *J. Geophys. Res. 87*, 10579-10597.

Sanders, C.O. and H. Kanamori (1984). A seismotectonic analysis of the Anza seismic gap, San Jacinto Fault Zone, Southern California, *J. Geophys. Res. 89*, 5873-5890.

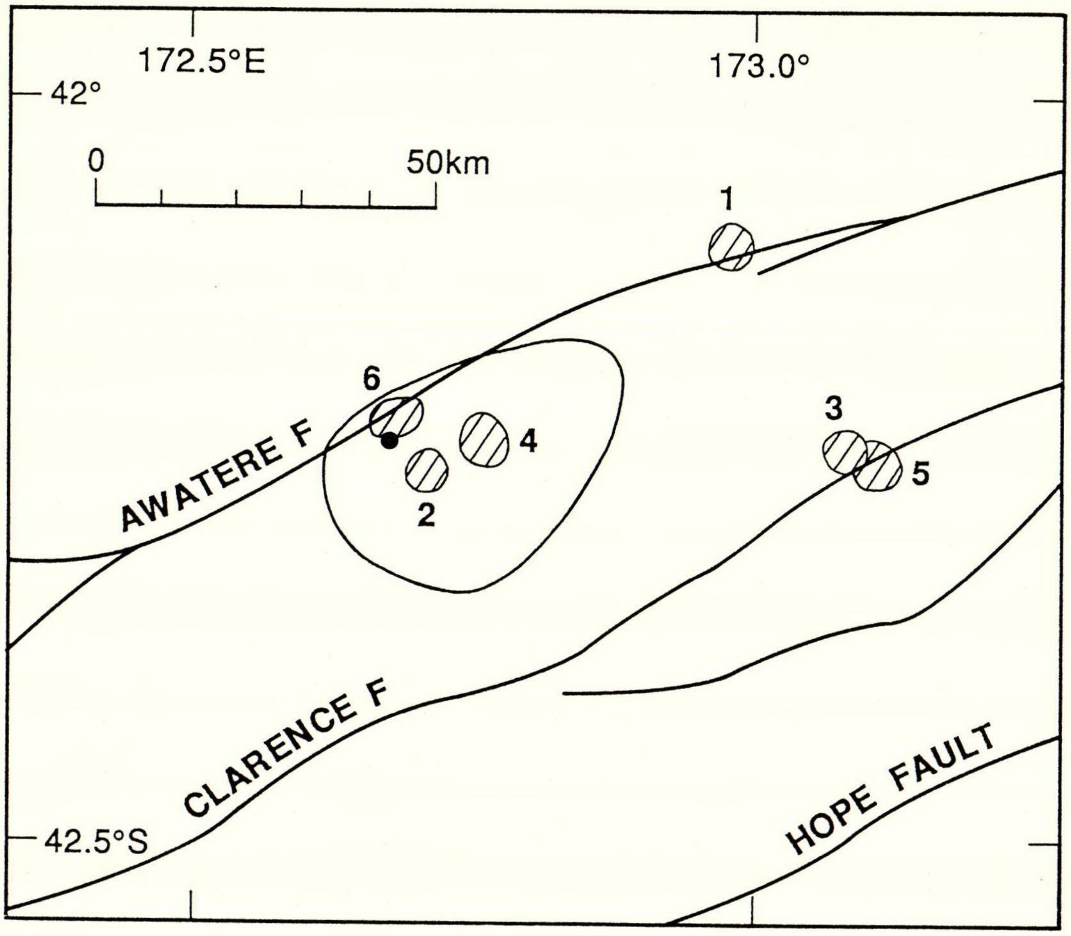

Figure 1. The Tennyson sequence. Numbered shaded regions show the location of precursory clusters. Note that cluster 1 is deep and not related to the sequence. The curve encircling clusters 2, 4, and 6 outlines the aftershock zone. The solid dot marks the mainshock.

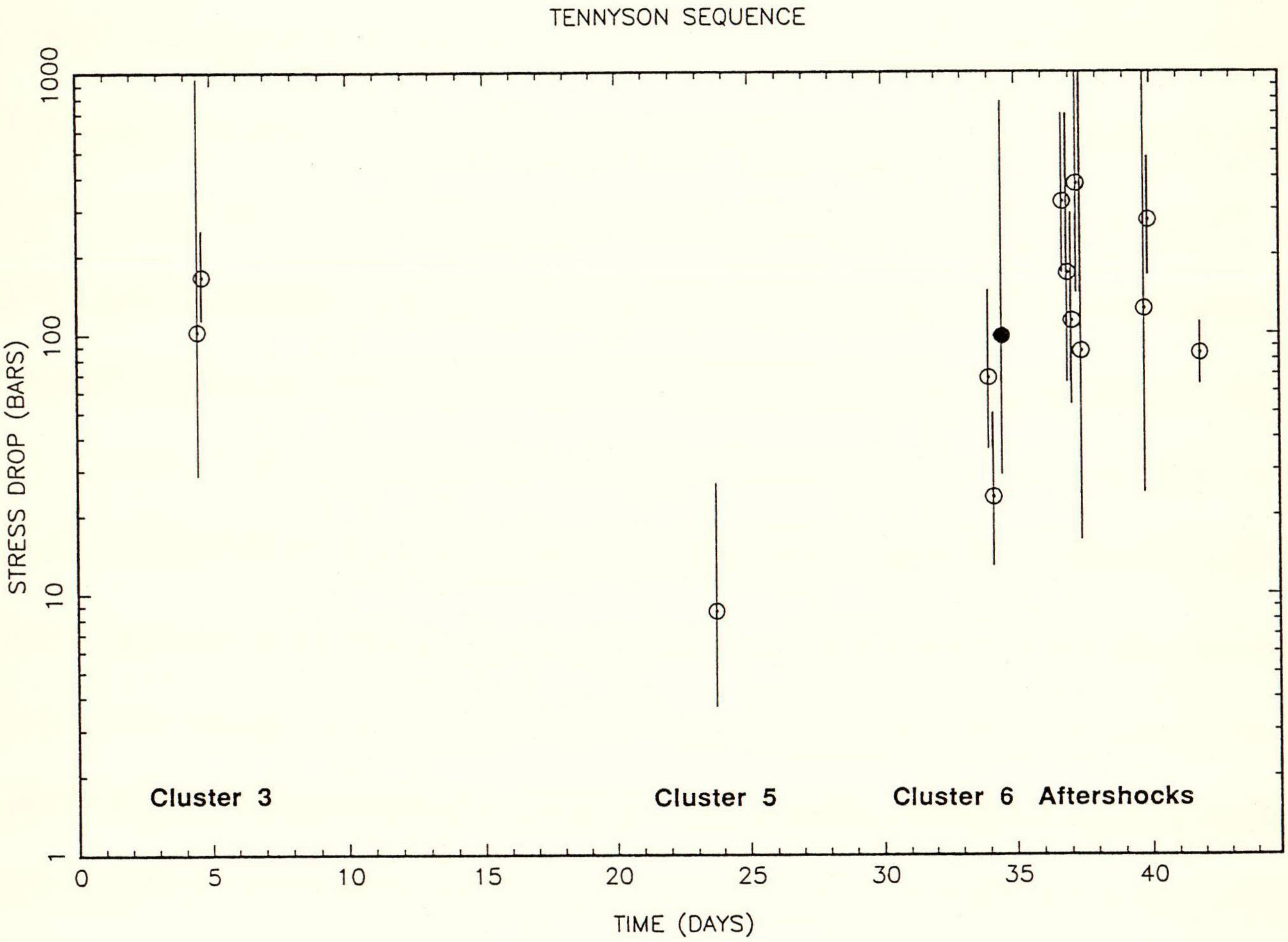

Figure 2. Stress drops of preshocks and aftershocks as a function of time. The cluster region locations are shown in Figure 1. The stress drop of the mainshock in marked by the solid circle and is only approximate.

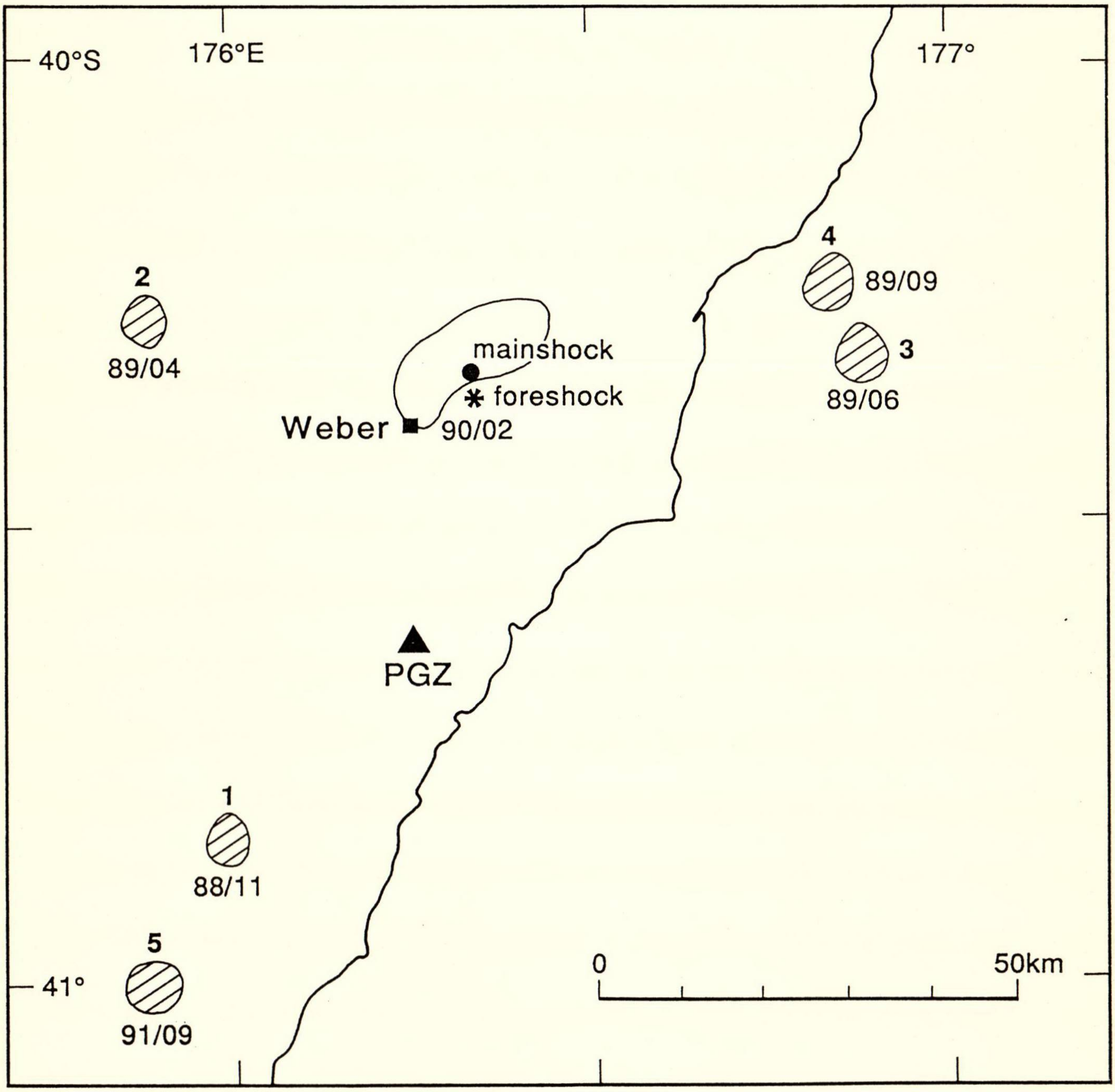

Figure 3. Location of the 1990 February Weber sequence. The solid circle marks the mainshock, the asterisk the immediate foreshock, and the curve outlines the aftershock zone. Numbered circles denote the location of cluster activity, each being labelled with the year and month of occurrence. EARSS station PGZ is marked with a solid triangle.